# A Homolytic Mechanism of O–O Bond Scission Prevails in the Reactions of Alkyl Hydroperoxides with an Octacationic Tetraphenylporphinato–Iron(III) Complex in Aqueous Solution

**Örn Almarsson[†] and Thomas C. Bruice***

*Contribution from the Department of Chemistry, University of California at Santa Barbara, Santa Barbara, California 93106*

*Received May 25, 1994[⊗]*

**Abstract:** The reaction of *t*-BuOOH with the novel octacationic, water soluble, nonaggregating, and non-$\mu$-oxo dimer forming *meso*-5,10,15,20-tetrakis(2,4,6-trimethyl-3,5-bis(α-*N*,*N*,*N*-trimethylammoniummethyl)phenyl)porphyrinatoiron-(III) dihydrate {(**3**)$Fe^{III}(X)_2$, where X = $H_2O$ and/or $HO^-$} was studied in buffered aqueous solutions between pH 0.9 and 12.1 at 30 °C and at constant ionic strength of 0.20. Minimal catalyst turnover conditions with $[t\text{-BuOOH}]_{initial} = 6.0 \times 10^{-5}$ M and $[(\mathbf{3})Fe^{III}(X)_2] = 1.9 \times 10^{-6}$ M were employed, in the presence and absence of excess 2,2′-azinobis(3-ethylbenzothiazoline-6-sulfonic acid) disodium salt (ABTS, with $[ABTS]_{initial} = 6.0 \times 10^{-3}$ M). ABTS serves to trap any hypervalent iron–porphyrin species as well as alkoxyl radical products. The reaction was established to be first-order in (**3**)$Fe^{III}(X)_2$ and *t*-BuOOH concentrations. The large number of positive charges on (**3**)$Fe^{III}(X)_2$ bring about competitive inhibition of the reaction by oxyanionic buffers. No general acid or general base catalysis is observed at any pH. A plot of the logarithms of $k_{ly}$ (the apparent second-order rate constants obtained by extrapolation to zero buffer concentration at each pH), vs pH was fit to a kinetic equation which takes into account three productive intermediates (**3**)$Fe^{III}(H_2O)$(*t*-BuOOH), (**3**)$Fe^{III}(H_2O)$(*t*-$BuOO^-$), and (**3**)$Fe^{III}(OH^-)$(*t*-$BuOO^-$). The major features of the pH-rate profiles of octacationic (**3**)$Fe^{III}(X)_2$ and tetraanionic tetrakis(2,6-dimethyl-3-sulfonatophenyl)porphyriniron(III) hydrate (**1**)$Fe^{III}(X)_2$ are much alike. Shifting of the profile toward lower pH values for (**3**)$Fe^{III}(X)_2$ is consistent with lowered $pK_a$ values for (**3**)$Fe^{III}(H_2O)_2$ when compared to (**1**)$Fe^{III}(H_2O)_2$. pH-Dependent second-order rate constants for reaction of *t*-BuOOH with the octacationic (**3**)$Fe^{III}(X)_2$ and tetraanionic (**1**)$Fe^{III}(X)_2$ are not greatly different. A plot of log $k_{ly}$ at pH 5.2 vs $pK_a$ of ROH in the reactions of (**3**)$Fe^{III}(X)_2$ with various alkyl and acyl hydroperoxides (ROOH) shows a break at $pK_a \sim 6$. At $pK_a$ (ROH) below 6, a large dependence of reaction rates on the $pK_a$ of ROH is observed ($-\beta_{1g} \sim 1.0$), indicative of a polar mechanism (heterolysis). Above $pK_a = 6$, a slight dependence on polar effects ($-\beta_{1g} \sim 0.2$) suggests a less polar transition state. The products from the reaction of *t*-BuOOH with (**3**)$Fe^{III}(X)_2$ are discussed in terms of four mechanisms: (a) heterolysis of *t*-BuOOH with a contribution from radical chain reactions; (b) a radical chain mechanism initiated by (**3**)$Fe^{IV}(X)(O)$; (c) Fenton chemistry involving (**3**)$Fe^{II}$ and (**3**)$Fe^{III}$ states; or (d) rate-limiting homolysis of the O–O bond in *t*-BuOOH.

## Introduction

The catalytic cycles of the heme-containing enzymes catalase[1] and peroxidases[2] are initiated when hydrogen peroxide converts the iron(III) protoporphyrin IX cofactor at the active sites to a iron(IV)–porphyrin $\pi$-cation radical species,[3] the so-called compound I. Compound I is two oxidation equivalents above the resting state of the enzymes (eq 1) and is therefore a product

$$(\text{porphyrin})Fe^{III}(OH_2) + H_2O_2 \xrightarrow{-H_2O} (\text{porphyrin}^{\bullet+})Fe^{IV}(=O) + H_2O \quad (1)$$

of net heterolytic cleavage of the HO–OH bond. The details of the mechanism of peroxide scission are to this time matters of much interest.[4-6] The question remains does the process involve simultaneous $2e^-$ transfer or stepwise two $1e^-$ transfers (Scheme 1). In our laboratory, studies with water soluble and non-$\mu$-oxo dimer forming tetraanionic tetraphenylporphyrinatoiron(III) complexes (**1**)$Fe^{III}(X)_2$ and (**2**)$Fe^{III}(X)_2$ (Chart 1) have afforded quantitative information on the dynamics and products

**Scheme 1**[4i]

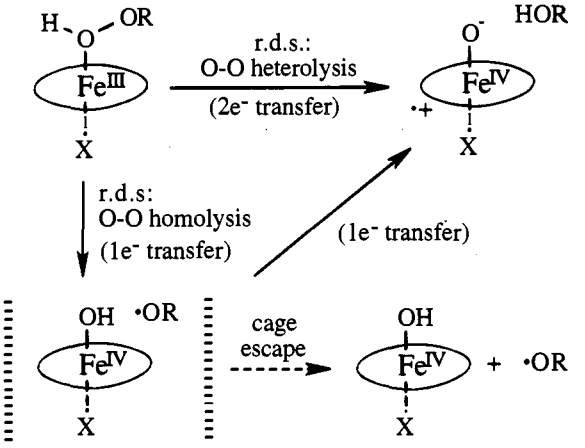


[†] In partial fulfillment of the Ph.D. degree in chemistry.

[⊗] Abstract published in *Advance ACS Abstracts*, March 15, 1995.

(1) Schonbaum, G. R.; Chance, B. In *The Enzymes*, 2nd ed.; Boyer, P. D., Ed.; Academic Press: New York, 1976; Vol. 13, pp 363–408.

(2) *Peroxidases in Chemistry and Biology*; Everse, J., Everse, K. E., Grisham, M. B., Eds.; CRC Press: Boca Raton, FL, 1991; Vol 2.

(3) (a) Dolphin, D.; Forman, A.; Borg, D. C.; Fajer, J.; Felton, R. H. *Proc. Natl. Acad. Sci. U.S.A.* **1971**, *68*, 614. (b) Moss, T. H.; Ehrenberg, A.; Beardon, A. J. *Biochemistry* **1969**, *8*, 4159. (c) Schulz, C. E.; Devaney, P. W.; Winkler, H.; Debrunner, P. G.; Doan, N.; Chiang, R.; Rutter, R.; Hager, L. P. *FEBS Lett.* **1979**, *103*, 102. (d) Roberts, J. E.; Hoffman, B. M.; Rutter, R.; Hager, L. P. *J. Biol. Chem.* **1981**, *256*, 2118.

0002-7863/95/1517-4533$09.00/0 

**Chart 1**

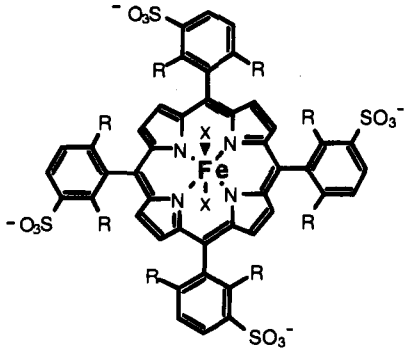

(1)$Fe^{III}(X)_2\{Na^+\}_4$ R = $CH_3$

(2)$Fe^{III}(X)_2\{Na^+\}_4$ R = Cl

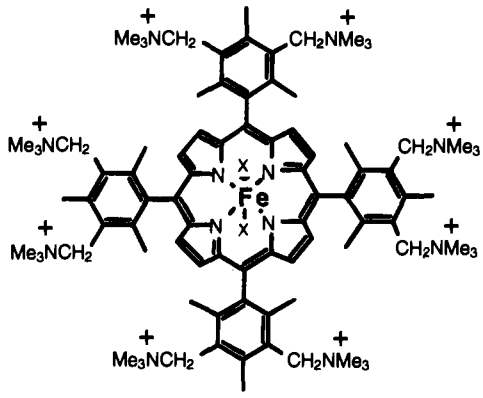

(3)$Fe^{III}(X)_2$ $\{Cl^-\}_8$

(X = $H_2O/HO^-$)

of the reactions of these iron(III) porphyrins with hydroperoxides in aqueous solution.[6a-o] Linear free energy plots of log of the second-order rate constants for reactions of ROOH vs p$K_a$ of ROH in the reactions of various alkyl- and acyl hydroperoxides (ROOH) with tetraanionic iron(III) porphyrin (1)$Fe^{III}(X)_2$ exhibit marked breaks in the slope, suggestive of two operating mechanisms.[6a] When $RO^-$ leaving groups are stable (such as carboxylate anions derived from peracid decomposition), a large sensitivity to polar effects is observed, in accord with the known heterolytic cleavage of the O–O bond in RC(=O)OOH. With the more weakly acidic alkyl RO–OH and $H_2O_2$, second-order rate constants were found to be much less sensitive to changes in the p$K_a$ of ROH, consistent with a nonpolar radical cleavage mechanism in the rate limiting step. The reactions of acyl and alkyl hydroperoxides in water are subject to neither general-acid nor general-base catalysis.[6a,d,h] Thus, the change in slope with leaving group stability cannot be associated with a change in transition state structure by way of an O'Ferrall–Jencks[7] (or MAR[8]) diagram. Products consistent with homolytic cleavage are obtained from the reactions of *tert*-butyl hydroperoxide {$(CH_3)_3COOH$}, cumyl hydroperoxide {$PhC(CH_3)_2OOH$}, and diphenyl carbomethoxymethyl hydroperoxide {$Ph_2C(CO_2Me)$-OOH} with (1)$Fe^{III}(X)_2$.[6d,h] Identities of the iron porphyrin intermediates {(**P**)$Fe^{II}$ and (**P**)$Fe^{IV}(X)(OH)$} do not support heterolysis of the alkyl hydroperoxide O–O bonds.[9,10] Although overall heterolysis of the peroxide substrates is observed in protoporphyrin IX catalyzed reactions in catalase and peroxidases, homolytic cleavage mechanisms for $H_2O_2$ and alkyl hydroperoxides are *not* necessarily inconsistent with the observed formation of {porphyrin$^{\bullet+}$}$Fe^{IV}(O)$ species (Scheme 1). An enzyme active site provides a means of detaining an $RO^\bullet$ intermediate to allow trapping "in the cage" {||(porphyrin)$Fe^{IV}$-(OH) $RO^\bullet$|| → ||(porphyrin$^{\bullet+}$)$Fe^{IV}(O)$ ROH||}. In water such trapping would be especially favorable in the case of hydrogen peroxide, since $HO^\bullet$ is a stronger oxidizing agent in water than most alkyl $RO^\bullet$ by more than 0.5 V ($\Delta\Delta G$ for one-electron reduction of $RO^\bullet$ vs $HO^\bullet$ > 11 kcal/mol).[11]

Reactions of tetraanionic (1)$Fe^{III}(X)_2$ and (2)$Fe^{III}(X)_2$ (Chart 1) with peroxides in water, with control of pH, ionic strength, and other parameters, have laid much of the foundation for our mechanistic arguments to this point.[5,6] Study of the reactions of iron(III) complexes of multicationic porphyrins with the same hydroperoxides would be useful since it has been held that the negative charges on (1)$Fe^{III}(X)_2$ and (2)$Fe^{III}(X)_2$ explains our lack of observation of general catalysis by oxyanion bases. We report here on the reactions of a novel octacationic *meso*-5,-10,15,20-tetrakis(2,4,6-trimethylphenyl-3,5-bis{α-*N,N,N*-trimethylammoniummethyl})porphyrinatoiron(III) dihydrate, (3)-$Fe^{III}(X)_2$ (Chart 1), with ROOH species. Like (1)$Fe^{III}(X)_2$ and (2)$Fe^{III}(X)_2$, (3)$Fe^{III}(X)_2$ is water soluble and does not aggregate nor form a μ-oxo dimer. In the previous paper in this issue, we found marked electronic effects of the peripheral quaternary ammonium ion substituents on the acid dissociation constants of the water ligands of (3)$Fe^{III}(H_2O)_2$. We now describe a study

(4) (a) Bruice, T. C. In *Mechanistic Principles of Enzymatic Activity*; Liebman, J. F., Greenberg, A., Eds.; VCH Publishers Inc.: Deerfield Beach, FL, 1988; Chapter 6, pp 227–277. (b) Ostovic, D.; Bruice, T. C. *J. Am. Chem. Soc.* **1988**, *110*, 6906. (c) Ostovic, D.; Bruice, T. C. *J. Am. Chem. Soc.* **1989**, *111*, 6511. (c) Yuan, L.-C.; Bruice, T. C. *Inorg. Chem.* **1985**, *24*, 986. (d) Yuan, L.-C.; Bruice, T. C. *J. Am. Chem. Soc.* **1986**, *108*, 1643. (e) Lee, W. A.; Yuan, L.-C.; Bruice, T. C. *J. Am. Chem. Soc.* **1988**, *110*, 4277. (f) Lee, W. A.; Bruice, T. C. *Inorg. Chem.* **1986**, *25*, 131. (g) Lee, W. A.; Bruice, T. C. *J. Am. Chem. Soc.* **1985**, *107*, 513. (h) Yuan, L.-C.; Bruice, T. C. *J. Am. Chem. Soc.* **1985**, *107*, 512. (i) Bruice, T. C. *Annals NY Acad. Sci.* **1986**, *471*, 83. (j) Balasubramanian, P. N.; Bruice, T. C. *J. Am. Chem. Soc.* **1986**, *108*, 5495.

(5) For reviews on reactions of hydroperoxides with water-soluble metallo tetraphenylporphyrins, see: (a) Bruice, T. C. *Acc. Chem. Res.* **1991**, *24*, 243. (b) Bruice, T. C. *Aldrich Chim. Acta* **1988**, *21*, 87.

(6) (a) Balasubramanian, P. N.; Lee, R. W.; Bruice, T. C. *J. Am. Chem. Soc.* **1989**, *111*, 8714. (b) Lindsay Smith, J. R.; Balasubramanian, P. N.; Bruice, T. C. *J. Am. Chem. Soc.* **1988**, *110*, 7411. (c) Balasubramanian, P. N.; Lindsay Smith, J. R.; Davies, M. J.; Kaaret, T. W.; Bruice, T. C. *J. Am. Chem. Soc.* **1989**, *111*, 1477. (d) Gopinath, E.; Bruice, T. C. *J. Am. Chem. Soc.* **1991**, *113*, 4657. (e) Zipplies, M. F.; Lee, W. A.; Bruice, T. C. *J. Am. Chem. Soc.* **1986**, *108*, 4433. (f) Murata, K.; Panicucci, R.; Gopinath, E.; Bruice, T. C. *J. Am. Chem. Soc.* **1990**, *112*, 6072. (g) Bruice, T. C.; Zipplies, M. F.; Lee, W. A. *Proc. Natl. Acad. Sci. U.S.A.* **1986**, *83*, 4646. (h) Gopinath, E.; Bruice, T. C. *J. Am. Chem. Soc.* **1991**, *113*, 6090. (i) Beck, M. J.; Gopinath, E.; Bruice, T. C. *J. Am. Chem. Soc.* **1993**, *115*, 421. (j) Castellino, A.; Bruice, T. C. *J. Am. Chem. Soc.* **1988**, *110*, 158. (k) He, G.-X.; Bruice, T. C. *J. Am. Chem. Soc.* **1991**, *113*, 2747. (l) Bruice, T. C.; Balasubramanian, P. N.; Lee, R. W.; Lindsay Smith, J. R. *J. Am. Chem. Soc.* **1988**, *110*, 7890. (m) Enona Gopinath, Ph.D. Thesis, UCSB, 1991. (n) Panicucci, R.; Bruice, T. C. *J. Am. Chem. Soc.* **1990**, *112*, 6063. (o) Castellino, A.; Bruice, T. C. *J. Am. Chem. Soc.* **1988**, *110*, 7512.

(7) (a) More O'Ferrall, R. A. *J. Chem. Soc. B* **1970**, 270. (b) Jencks, W. P. *Chem. Rev.* **1972**, *72*, 705.

(8) Bruice, T. C. *Annu. Rev. Biochem.* **1976**, *45*, 331.

(9) On the other hand, the nature and stereochemistry of epoxidation products of norbornene with iron tetraphenylporphyrins in organic solvents has been taken as evidence for heterolytic scission of ROOH. See ref 10. See, also, however: refs 4b and 4c.

(10) Traylor, T. G.; Tsuchiya, S.; Byun, Y.-S.; Kim, C. *J. Am. Chem. Soc.* **1993**, *115*, 2775.

(11) (a) Sawyer, D. T.; Roberts, J. L. *Acc. Chem. Res.* **1988**, *21*, 469. (b) Barton, D. H. R.; and Sawyer, D. T. In *The Activation of Dioxygen and Homogeneous Catalytic Oxidation*; Barton, D. H. R., Martell, A. E., Sawyer, D. T., Eds.; Plenum: New York, 1993; Chapter 1.

of the kinetics and products of reaction of *t*-BuOOH and (**3**)-$Fe^{III}(X)_2$ in buffered aqueous solutions at 30 °C and $\mu = 0.2$ between pH 0.9 and 12.1.

## Experimental Section

**Materials.** The synthesis of (**3**)$Fe^{III}(X)_2$ dihydrate is described in the previous paper in this issue. *tert*-Butyl hydroperoxide (70% aqueous solution), cumyl hydroperoxide (neat), 85% 3-chloroperbenzoic acid (*m*-CPBA), and 85% *p*-nitroperbenzoic acid were purchased from Aldrich. Perbenzoic acid was synthesized by basic hydroperolysis of benzoyl peroxide.[12] 4-Chloroperbutyric acid was synthesized from 4-chlorobutyric acid and 50% hydrogen peroxide (Fisher) by the method of Silbert et al.[13] All commercial hydroperoxides and peracids were used as received but standardized for peroxide content prior to use.[14] Diphenyl carbomethoxymethyl hydroperoxide {$Ph_2C(CO_2Me)OOH$} and diphenyl cyanomethyl hydroperoxide {$Ph_2C(CN)OOH$} were available from a previous study.[6h] Kinetic and product studies were performed in double glass distilled water. Buffer materials of highest purity available were used to prepare buffered solutions, which were kept in aqueous EDTA treated plastic bottles prior to use. Phosphate and borate stock solutions were passed through a Chelex column prior to dilution and pH adjustment with fresh samples of 1 M NaOH (prepared with degassed doubly distilled water) or 1 M HCl. Radiometer model 26 pH-meter and Fisher 13-620-280 micro glass electrode were used for proton activity measurements. No sodium ion correction is necessary up to pH 12.5. $NaNO_3$ (3 M) (for adjustment of ionic strength) was prepared from reagent grade material and passed through a Chelex column prior to use. 2,2′-Azinobis(3-ethylbenzothiazoline-6-sulfonic acid) disodium salt (ABTS·$Na_2$, henceforth abbreviated as ABTS) was prepared[6d] from the commercially available diammonium salt (ABTS·$\{NH_4\}_2$) (Sigma-Aldrich).

**Instrumentation.** UV–visible absorption spectra were obtained on a CARY-14 spectrometer, interfaced with a Gateway 2000 PC computer running On-Line Instruments (OLIS, Bogart, GA) software. At pH values over 6.5, samples were prepared in a glovebox under nitrogen atmosphere in degassed, doubly distilled water. *t*-BuOOH and aqueous NaOH at pH over 10.4 were placed in the top compartment of a Thunberg cuvette assembly with the remaining components present in the cuvette. The contents were allowed to equilibrate at 30 °C before rapid mixing of the compartments immediately prior to assay. Fast reactions of peracids were conducted on a OLIS-RSM stopped flow spectrophotometer at 30 °C with the standard OLIS-supplied software. Kinetics were followed by monitoring the appearance of $ABTS^{\bullet+}$ at 660 nm as well as following changes in absorbance at other wavelengths and by using the supplied routine for fitting kinetics at multiple wavelengths simultaneously.[15] Product analysis from reactions of *t*-BuOOH with (**3**)$Fe^{III}(X)_2$ was achieved by injecting 0.5 μL of the mixtures from completed (>6 half-lives) reactions onto a Varian 3700 series gas chromatograph, fitted with a QC2/BP-1 (25 × 0.32 mm i.d., SGE) capillary column at 30 °C, with appropriate sample splitting and flame ionization detection. Reactions were initiated by adding *t*-BuOOH to an initial concentration of $7.1 \times 10^{-4}$ M to solutions of $[(\mathbf{3})Fe^{III}(X)_2] = 1.9 \times 10^{-6}$ M in (i) 0.01 M HCl (pH 2.0), (ii) 50 mM acetate buffer (pH 5.6), and (iii) 50 mM carbonate buffer (pH 9.3). Ionic strength was maintained at 0.2, as before, and reactions were allowed to proceed until depletion of the oxidant. Product yields, based on the amount of *t*-BuOOH, were calculated from peak areas on a Hewlett Packard HP3392A integrator, using standard response curves created from assays of known concentrations of each major product.

## Results

In the reactions of hydroperoxides with iron(III) porphyrin catalysts at low porphyrin and substrate concentrations, the catalyst is not saturated with peroxide. When [hydroperoxide] initially exceeds [catalyst], the kinetic order in the reactants is obtained as follows. Increase in [hydroperoxide] does not increase the pseudo-first-order rate constant ($k_{obsd}$), but it does increase the concentration of product formed with time {there is an increase in the initial rate}. The reaction is first order in [hydroperoxide] if a plot of initial rate ($k_i$) vs [hydroperoxide] is linear. Increase in [catalyst] increases $k_{obsd}$ and the reaction is first order in [catalyst] if a plot of $k_{obsd}$ vs [catalyst] is linear. The (pH- and other variable dependent) apparent second order rate constants ($k_{ly}$) are obtained as the slope of the plot of $k_{obsd}$ vs [catalyst] at fixed pH values or for those pH values where only one porphyrin concentration is employed, $k_{ly} = k_{obsd}/$[catalyst].

**Kinetics of the reactions of *tert*-butyl hydroperoxide (*t*-BuOOH) with (3)$Fe^{III}(X)_2$** were determined spectrophotometrically as previously described[6] in buffered aqueous solutions at 30 °C, constant ionic strength ($\mu = 0.20$ with $NaNO_3$) and over a range of pH from 0.9 to 12. Trapping of hypervalent iron species as well as putative alkoxyl radical products, was accomplished by addition of a large excess of 2,2′-azinobis(3-ethylbenzothiazoline-6-sulfonic acid) disodium salt (ABTS). The first-order appearance of the absorption at 660 nm due to $ABTS^{\bullet+}$ formation was used to monitor the progress of the reaction. Two molecules of ABTS are oxidized to $ABTS^{\bullet+}$ for each *t*-BuOOH consumed, regardless of the nature of the O–O bond cleavage step (eq 2a,b). Pseudo-first-order conditions of

$$(\mathbf{3})Fe^{III} + (CH_3)_3COOH \longrightarrow (\mathbf{3}^{\bullet+})Fe^{IV}(O) + (CH_3)_3COH$$

$$\xrightarrow[2ABTS^{\bullet+}]{2ABTS + 2H^+} (\mathbf{3})Fe^{III} + H_2O \quad (2a)$$

$$(\mathbf{3})Fe^{III} + (CH_3)_3COOH \longrightarrow \| (\mathbf{3})Fe^{IV}(OH) + (CH_3)_3CO\cdot \|$$

$$\xrightarrow[2ABTS^{\bullet+}]{2ABTS + 2H^+} (\mathbf{3})Fe^{III} + (CH_3)_3COH + H_2O \quad (2b)$$
(and others)

$[ABTS]_{initial} = 6.0 \times 10^{-3}$ M $\gg [t\text{-BuOOH}]_{initial} = 6.0 \times 10^{-5}$ M $> [(\mathbf{3})Fe^{III}(X)_2] = 1.1 \times 10^{-6}$ M were employed. The reactions are found to be zero order in ABTS (eqs 3 and 4).

$$d[ABTS^{\bullet+}]/dt = k_{ly}[(\mathbf{3})Fe^{III}(X)_2][t\text{-BuOOH}]_i \quad (3)$$

$$k_{obsd} = k_{ly}[(\mathbf{3})Fe^{III}(X)_2] \quad (4)$$

Appearance of $ABTS^{\bullet+}$ followed the first-order rate law at pH 3.6 to 9.4. At pH below 3.6, the first-order appearance of $ABTS^{\bullet+}$ is concurrent with a slower zero-order $ABTS^{\bullet+}$ formation due to oxidation of ABTS by oxygen. Above pH 9.4, reaction of $ABTS^{\bullet+}$ with $HO^-$ results in appearance and disappearance of $ABTS^{\bullet+}$ (660 nm) *via* two sequential first order processes. The time courses for the reactions at each pH and at each buffer concentration were fit to the appropriate expression for two sequential first-order reactions {ABTS going to $ABTS^{\bullet+}$ with $k_1$ and $ABTS^{\bullet+}$ going to $ABTS^{2+}$ with $k_2$}. The value of $k_1 = k_{obsd}$ for oxidation of (**3**)$Fe^{III}(X)_2$ by *t*-BuOOH. Figure 1 shows the dependence of $k_{obsd}$ on the concentration of (**3**)$Fe^{III}(X)_2$ ($1 \times 10^{-7}$–$5.4 \times 10^{-6}$ M) at varying constant values of pH, with $[t\text{-BuOOH}]_i = 6.0 \times 10^{-5}$ M. A linear dependence of the observed pseudo-first-order rate constants on iron(III) porphyrin concentration is observed at five pH values between pH 2.1 and 10.4. The slopes of the plots equal $k_{ly}$, unless dependence on buffer concentration is observed (*vide infra*). The order in peroxide was asessed by varying the initial

(12) Ogata, Y.; Sawaki, Y. *Tetrahedron* **1967**, *23*, 3327.
(13) Silbert, L. S.; Sieel, E.; Swern, D. *J. Org. Chem.* **1962**, *27*, 1336.
(14) Bruice, T. C.; Noar, J. B.; Ball, S.; Venkataram, U. V. *J. Am. Chem. Soc.* **1983**, *105*, 2452.
(15) The method of successive integration was developed by OLIS Instruments, Bogart, GA {*Anal. Instr.* **1987**, *16*, 345}. The simultaneous multiple wavelength fitting procedure is based on factor analysis, global fitting, and spectral reconstruction, as provided with the OLIS-RSM instrument.

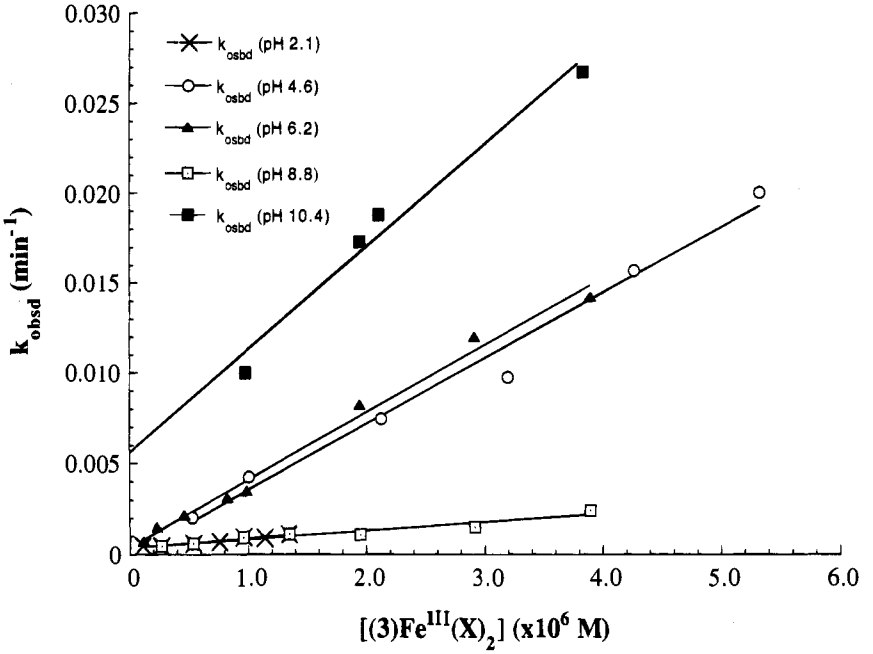


**Figure 1.** Plots of pseudo-first order reaction rates ($min^{-1}$) for reactions of *t*-BuOOH ($[t\text{-BuOOH}]_i = 6.0 \times 10^{-5}$ M) and (**3**)$Fe^{III}(X)_2$ at 30 °C as a function of porphyrin concentration. At the five pH values, porphyrin concentrations range between $1 \times 10^{-7}$ and $5.4 \times 10^{-6}$ M, and, in each case, $\mu = 0.2$ and total buffer concentrations are 0.1 M, where applicable. Linear regression analysis yields straight lines with slopes representing values of the second order rate constant for the reaction at 0.1 M buffer. The rates at the *y*-intercepts are nearly zero, except in the experiment at pH 10.4. The plots demonstrate a first-order dependence of the reaction rate on porphyrin concentration.

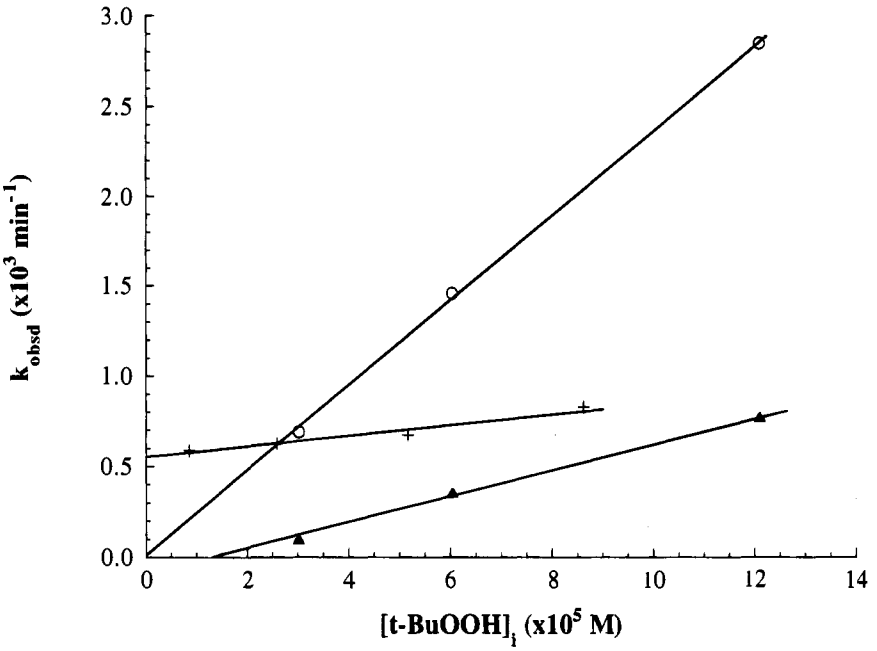


**Figure 2.** Initial slopes of kinetic traces vs initial *tert*-butyl hydroperoxide concentration ($[t\text{-BuOOH}]_i$), at three pH values. The porphyrin concentrations were (a) pH 2.1; $1.1 \times 10^{-6}$ M (crosses); (b) pH 6.2, $9.6 \times 10^{-7}$ M (circles); and (c) pH 9.3, $9.6 \times 10^{-6}$ M (triangles). The plots establish a first-order dependence of reaction rates on initial *tert*-butyl hydroperoxide concentration.

concentration of *t*-BuOOH at a constant [(**3**)$Fe^{III}(X)_2$] and plotting the initial slopes of the kinetic traces vs $[t\text{-BuOOH}]_i$ (Figure 2). A first-order dependence of $k_i$ (initial rate) on $[t\text{-BuOOH}]_i$ was established at three pH values (2.1, 6.2, and 9.3). The effects of ionic strength (Table 1) and buffer concentration on rate were investigated. Table 1 shows the dependence of $k_{1y}$ on ionic strength ($\mu$ = 0.075 and 0.75). Values of $k_{1y}$ show slight increases with increasing ionic strength, but the changes are usually within 2-fold over a 10-fold change in ionic strength. There are two exceptions in Table 1, where larger rate enhancements are observed. In 0.1 M cacodylate buffer at pH 6.2, a 10-fold increase in ionic strength causes the rate to increase 6.4-fold. In 0.1 M phosphate buffer at pH 6.7, a 10-fold increase in ionic strength causes a rate increase of 4.8-fold. At ionic strengths above 0.75, precipitation was observed, rendering the observed rate constants unreliable. The identity of the precipitate (fine green needles) is likely that of a salt of the ABTS radical cation ($ABTS{\cdot}Na_2X$, where X is an undetermined counteranion).

Studies of the inhibition of rates of reaction of *t*-BuOOH with

**Table 1.** Apparent Second Order Rate Constants for Reactions of *t*-BuOOH with (**3**)$Fe^{III}(X)_2$ at 30 °C as a Function of Ionic Strength[a]

| $\mu$ (M)[a] | pH | buffer[b] | $k^c$ ($M^{-1}$ $s^{-1}$) | rel $k^d$ | $\mu$ (M)[a] | pH | buffer[b] | $k^c$ ($M^{-1}$ $s^{-1}$) | rel $k^d$ |
|---|---|---|---|---|---|---|---|---|---|
| 0.04 | 2.1 | (HCl) | 18.1 | 1.0 | 0.4 | 6.1 | cacodylate | 74.9 | 3.2 |
| 0.2 | 2.1 | (HCl) | 27.2 | 1.5 | 0.75 | 6.1 | cacodylate | 150 | 6.4 |
| 0.075 | 3.1 | formate | 18.3 | 1.0 | 0.075 | 6.7 | phosphate | 65.0 | 1.0 |
| 0.75 | 3.1 | formate | 25.0 | 1.3 | 0.4 | 6.7 | phosphate | 91.6 | 1.4 |
| 0.1 | 4.6 | acetate | 45.0 | 1.0 | 0.75 | 6.7 | phosphate | 312 | 4.8 |
| 0.5 | 4.6 | acetate | 55.1 | 1.2 | 0.075 | 10.4 | (NaOH) | 250 | 1.0 |
| 0.075 | 6.1 | cacodylate | 23.3 | 1.0 | 0.75 | 10.4 | (NaOH) | 398 | 1.6 |

[a] Ionic strength, maintained with 3 M $NaNO_3$. [b] Except in the cases of HCl and NaOH, total buffer concentration is 100 mM. [c] Apparent second-order rate constant, obtained by dividing the pseudo-first-order constants ($k_{obsd}$ in $s^{-1}$) by the porphyrin concentration (M). [d] At each pH, values of $k$ at the lowest ionic strength are taken as a relative rate of 1.0.

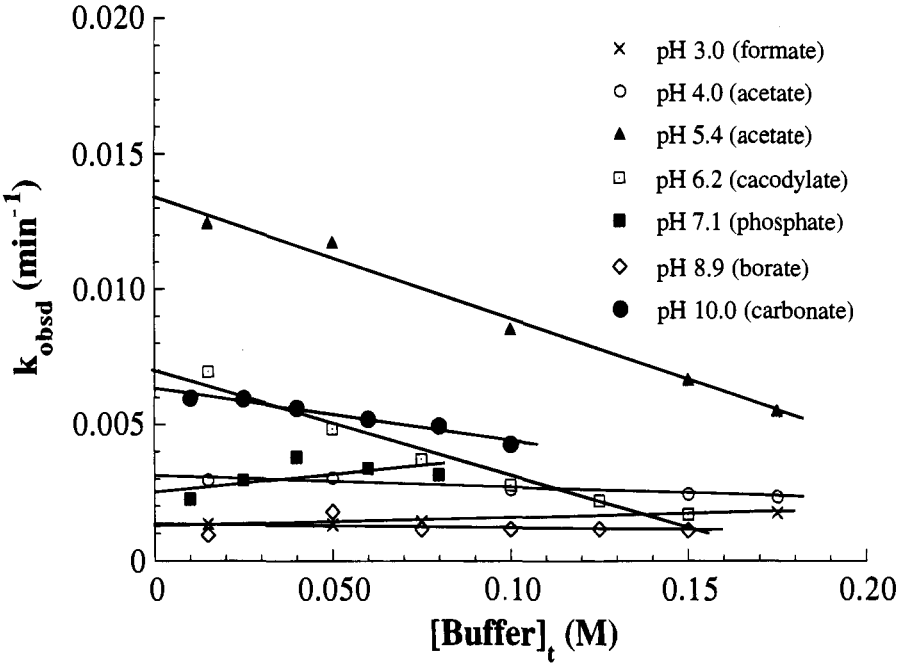


**Figure 3.** Plots of pseudo-first-order reaction rates ($min^{-1}$) for reactions of *t*-BuOOH and (**3**)$Fe^{III}(X)_2$ at 30 °C as a function of total buffer concentration ($[B]_t = [B] + [BH^+]$). In each case, $\mu = 0.2$ and $[(\mathbf{3})Fe^{III}(X)_2] = 1.9 \times 10^{-6}$ M. The intercept of the straight lines obtained from linear regression analysis yield pseudo-first-order rate constants at zero buffer concentration. The value at the intercept is divided by 60 (s/min) as well as the porphyrin concentration to give second-order rate constants $k_{ly}$ ($M^{-1}$ $s^{-1}$).

(**3**)$Fe^{III}(X)_2$ by oxyanionic buffers were carried out at an ionic strength of 0.2. Plots of observed pseudo-first-order rate constants ($k_{obsd}$) vs total buffer concentration, such as those shown in Figure 3, were constructed at each pH value in every buffer system employed. Inhibition is more pronounced at pH values where the equilibrium in a given buffer system {$BH \rightleftharpoons B^- + H^+$} lies on the side of $B^-$ ($pH > pK_a$). The buffer-independent second-order rate constants, $k_{ly}$, for the reaction of (**3**)$Fe^{III}(X)_2$ with *t*-BuOOH are obtained by extrapolation of plots, such as those of Figure 3, to zero buffer concentration and dividing the intercept by the concentration of iron(III) porphyrin.

Figure 4 shows a plot of log $k_{ly}$ vs pH. As is the case in the reactions of (**1**)$Fe^{III}(X)_2$,[6d] the pH dependence of the experimental values for $k_{ly}$ for the reaction of (**3**)$Fe^{III}(X)_2$ with *t*-BuOOH can be simulated by a combination of four pathways, which are related through the acid dissociation constants of the catalyst and substrate (Scheme 2). The four contributing pathways are shown in Scheme 3.[6d,h] By use of the steady-state assumption in the intermediates $\mathbf{PH_2}^+$, **PH**, $\mathbf{P}^-$ (Scheme 4), one arrives at the kinetic expressions of eqs 5–8.[6d,f] The derived equations for each pathway are given in eqs 5–7. Path A in Scheme 3 is represented by eq 5, paths B and C are embodied in eq 6, and pathway D is described by eq 7. Each

**Scheme 2**

$$t\text{-BuOOH} \underset{+H^+}{\overset{-H^+}{\rightleftharpoons}} t\text{-BuOO}^- \quad K_b = 1.6 \times 10^{-13}$$

$$(\mathbf{3})Fe^{III}(H_2O)_2 \underset{+H^+}{\overset{K_{a1}\ -H^+}{\rightleftharpoons}} (\mathbf{3})Fe^{III}(H_2O)(OH) \underset{+H^+}{\overset{K_{a2}\ -H^+}{\rightleftharpoons}} (\mathbf{3})Fe^{III}(OH)_2$$

**Scheme 3**

$$\text{A: } (\mathbf{3})Fe^{III}(H_2O)_2{}^+ \underset{k_{-1}}{\overset{k_1[ROOH]}{\rightleftharpoons}} \mathbf{PH_2}^+ \xrightarrow{k_2} \{(\mathbf{3})Fe^{IV}(H_2O)(OH)\}^+$$

$$\text{B: } (\mathbf{3})Fe^{III}(H_2O)_2{}^+ \underset{k_{-1}}{\overset{k_1[ROOH]}{\rightleftharpoons}} \mathbf{PH_2}^+ \underset{+H^+}{\overset{K_{a3}\ -H^+}{\rightleftharpoons}} \mathbf{PH} \xrightarrow{k_4} (\mathbf{3})Fe^{IV}(OH)_2$$

$$\text{C: } (\mathbf{3})Fe^{III}(H_2O)(OH) \underset{k_{-3}}{\overset{k_3[ROOH]}{\rightleftharpoons}} \mathbf{PH} \xrightarrow{k_4} (\mathbf{3})Fe^{IV}(OH)_2$$

$$\text{D: } (\mathbf{3})Fe^{III}(OH)_2{}^- \underset{+OH^-}{\overset{K_D\ -OH^-}{\rightleftharpoons}} (\mathbf{3})Fe^{III}OH^+ \underset{k_{-5}}{\overset{k_5[ROO^-]}{\rightleftharpoons}} \mathbf{P}^- \xrightarrow{k_6} (\mathbf{3})Fe^{IV}(OH)(O)_2{}^-$$

contribution can be appreciated by inspection of Figure 4, where plots of each function in eqs 5–7 are shown as lines, overlaid on the dashed pH-rate profile. Equation 8 is a combination of

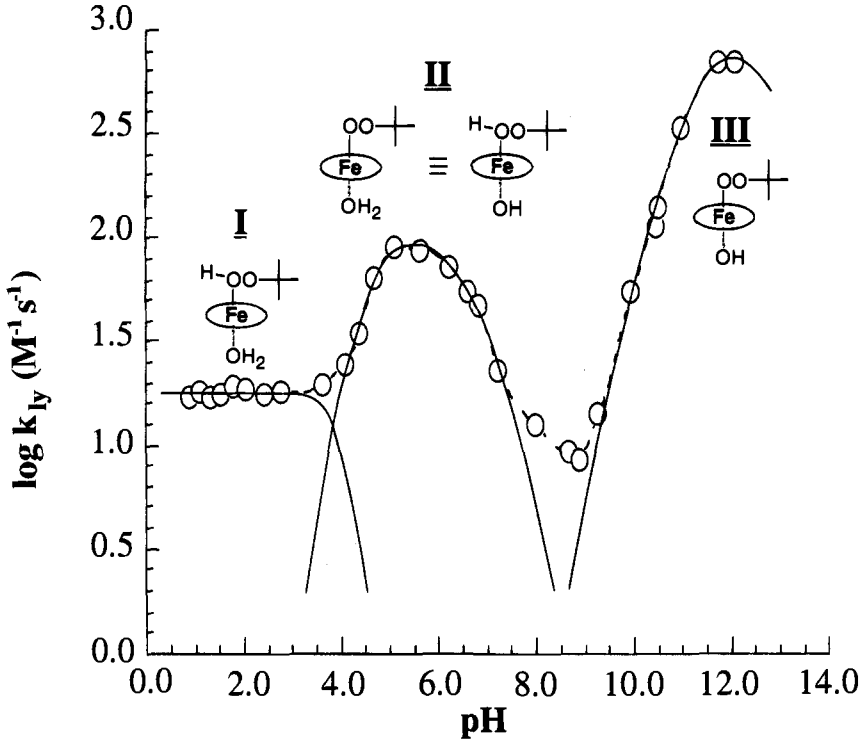


**Figure 4.** Plot of the logarithm of second-order rate constants {pH-rate profile} for the reactions of *t*-BuOOH and (**3**)$Fe^{III}(X)_2$ at 30 °C, $\mu = 0.2$. Each rate, $k_{ly}$ (in units of $M^{-1}$ $s^{-1}$), is obtained from the intercept of a buffer dilution plot, as described in the legend to Figure 3. Initial *t*-BuOOH concentration is $6.0 \times 10^{-5}$ M. The points are experimental, whereas the dotted line is a fit of the experimental points to a sum of eqs 5–7 (i.e., eq 8, see text). The solid lines, labeled I–III, represent the contribution of each equation separately.

**Scheme 4**

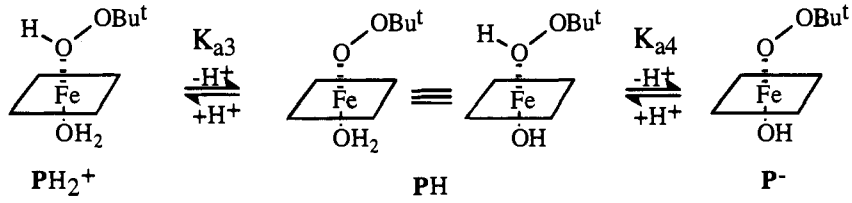


the rate expressions and was employed to fit the data points of log $k_{ly}$ vs pH over the entire pH range. In the plateau region at

$$k_{ly} = \frac{k_2 k_1}{k_2 + k_{-1}}\left\{\frac{a_H}{a_H + K_{a1}}\right\} \quad \{I\} \qquad (5)$$

$$k_{ly} = \frac{\frac{k_2 k_1}{k_2 + k_{-1}}\left\{\frac{k_4 K_{a3} a_H^{\,2}}{k_2} + \frac{k_4 k_3 K_{a1} K_{a3} a_H}{k_1 k_2}\right\}}{\left\{a_H^{\,2} + \frac{(k_4 + k_{-3}) a_H K_{a3}}{(k_2 + k_{-1})} + \frac{(k_6 + k_{-5}) K_{a3} K_{a4}}{(k_2 + k_{-1})}\right\}(a_H + K_{a1})} \quad \{II\} \qquad (6)$$

$$k_{ly} = \frac{\left\{\frac{k_6 k_5 K_D K_{a2} K_B}{(k_6 + k_{-5}) K_w}\right\} a_H}{(a_H + K_{a2})(K_b + a_H)} \quad \{III\} \qquad (7)$$

$$\text{rate} = \{I\} + \{II\} + \{III\} \qquad (8)$$

low pH (pH < 3.2), where $k_{ly}$ is independent of proton activity, the profile is described by eq 5 (pathway A). Products are derived from $PH_2^+$ (Scheme 4). At zero buffer concentration at pH below 3.2, the second order rate constant $k_{ly}$ (17.7 $M^{-1}$ $s^{-1}$) is simply a function of rate constants $k_1$, $k_{-1}$, and $k_2$ (eq 5).

In the intermediate pH region (3.3 to 8.9), the pH-rate profile can be described by two overlapping bells (eq 6, pathways B and C in Scheme 3). The complex from which *t*-BuOOH decomposition ensues {**PH** in Scheme 4} can form via pathway B or C. The final part of the pH-rate profile (pH > 9.0) is fit by eq 7, which defines a bell shaped curve. At high pH, the reacting complex is (**3**)$Fe^{III}(OH)$(*t*-$BuOO^-$) {$\mathbf{P}^-$ in Scheme 4} and forms via path D in Scheme 3. A decrease in reaction rate at very high pH is due to $HO^-$ competing with peroxide substrate for ligation to the iron.

Table 2 contains the kinetic and thermodynamic parameters obtained from fitting of the experimental points of the profile of Figure 4 to eq 8. Some interesting observations are made upon inspection of the composite kinetic terms in Table 2. (i) The true second order rate constant at low pH $\{k_1 k_2/(k_2 + k_{-1})\}$ is slightly more than 3-fold larger for the reaction of *t*-BuOOH with (**3**)$Fe^{III}(H_2O)_2$ than with (**1**)$Fe^{III}(H_2O)_2$. (ii) Two terms, $k_4 K_{a3}/k_2$ and $k_3/k_1$ are essentially unaffected by the difference in internal cationic and anionic environments of (**3**)$Fe^{III}(H_2O)_2$ and (**1**)$Fe^{III}(H_2O)_2$. (iii) The kinetically apparent value of $K_{a1}$ is ~5-fold larger than that determined by spectrophotometric titration ($K_a = 1.6 \times 10^{-6}$ M at $\mu = 0.2$, see previous paper in this issue), whereas the kinetic value of $K_{a2}$ ($6.3 \times 10^{-12}$ M) is almost exactly one order of magnitude smaller than obtained by spectral titration ($7.4 \times 10^{-11}$ M, see previous paper in this issue). (iv) The composite term in Table 2 which includes the

**Table 2.** Kinetic and Thermodynamic Parameters Obtained from Fitting of the pH Rate Profiles for Reaction of *t*-BuOOH with Two Iron(III) Tetraphenylporphyrins in Water

| term[a] | value determined for (3)$Fe^{III}(X)_2$[b] | value determined for (1)$Fe^{III}(X)_2$[c] |
|---|---|---|
| $(k_1k_2/(k_2 + k_{-1})$ | 17.7 | 5.0 |
| $(k_4/k_2)K_{a3}$ | $9.0 \times 10^{-5}$ | $1.4 \times 10^{-4}$ |
| $k_3/k_1$ | 0.42 | 0.43 |
| $(k_4 + k_{-3})K_{a3}/(k_2 + k_{-1})$ | $1.3 \times 10^{-7}$ | $5.5 \times 10^{-7}$ |
| $(k_6 + k_{-5})K_{a4}/(k_4 + k_{-3})$ | $1.5 \times 10^{-16}$ | $1.1 \times 10^{-8}$ |
| $K_{a1}$ | $7.7 \times 10^{-6}$ | $1.8 \times 10^{-7}$ |
| $k_6k_5K_D/(k_6 + k_{-5})$ | 0.83 | 71.1 |
| $K_{a2}$ | $6.3 \times 10^{-12}$ | $1.2 \times 10^{-11}$ |

[a] See eqs 5–7, constants are in units of M and $s^{-1}$. [b] This study. [c] Reference 6d. See Chart 1 for the structures (3)$Fe^{III}(X)_2$ and (1)$Fe^{III}(X)_2$.

**Table 3.** Products from Reactions of *t*-BuOOH with (3)$Fe^{III}(X)_2$ at Three Values of pH

| pH | ABTS[a] | % acetone[b,c] | % *t*-BuOH[b,d] | Σ%[e] | A/B[f] |
|---|---|---|---|---|---|
| 2.0 | + | 15 | 77 | 92 | 0.19 |
| 2.0 | − | 57 | 43 | 100 | 1.3 |
| 5.6 | + | 10 | 93 | 103 | 0.11 |
| 5.6 | − | 73 | 15 | 87 | 4.9 |
| 9.3 | + | 32 | 96 | 128 | 0.33 |
| 9.3 | − | 100 | 17 | 117 | 5.9 |

[a] +, $[ABTS]_i = 7 \times 10^{-3}$ M; −, ABTS was absent. [b] Percent yields by capillary GC. [c] ±5% (1 $\sigma_{n-1}$ for four determinations). [d] ±4% (1 $\sigma_{n-1}$ for four determinations). [e] Sum of acetone and *t*-BuOH yields. [f] Ratio of acetone to *t*-BuOH yields.

dissociation constant $K_D$, reflecting hydroxide ion ligation to the iron(III), is smaller by approximately two orders of magnitude in the case of (3)$Fe^{III}(X)_2$ compared with (1)$Fe^{III}(X)_2$. We defer further interpretation of the factors responsible for these differences to the Discussion section.

**Product analyses from reactions of *t*-BuOOH and (3)$Fe^{III}(X)_2$** were performed by direct gas chromatographic separation. The identities and yields of the products *t*-BuOH and acetone at three different pH values, in the absence and presence of ABTS, are summarized in Table 3. Di-*tert*-butyl peroxide could not be detected in any run. Acetone and *t*-BuOH account for >87% of the mass balance (see Σ% in Table 3), if it is assumed that $(CH_3)_3CO^{\bullet} + {}^{\bullet}OH \rightarrow (CH_3)_2C{=}O + CH_3OH$ (*vide infra*). Although methanol was also detected in the GC analyses, we find that at $[t\text{-BuOOH}] \simeq 10^{-5}$ M it is difficult to quantitatively determine the percent yield of $CH_3OH$. In one instance (pH 2.0) where ABTS is absent, the yield of *t*-BuOH is greater than that obtained at higher pH values. We have calculated, in addition to percent yields of *t*-BuOH and acetone and the sum of yields, the ratio of the yields of acetone to *t*-BuOH (A/B in Table 3). Importantly, the A/B ratio is always significantly larger than 1.0 when ABTS is absent. In contrast, when ABTS is present this ratio is always less than 0.33.

**Linear Free Energy Relationship of log $k_{ly}$ vs p$K_a'$ of ROH for Reactions of (3)$Fe^{III}(X)_2$ with ROOH.** Figure 5 shows a plot of log $k_{ly}$ for reactions of (3)$Fe^{III}(H_2O)(OH)$ (pH 5.2) and (1)$Fe^{III}(H_2O)(OH)$ (pH 6.7) {the latter from a previous study[6a]} with various alkyl and acyl hydroperoxides vs p$K_a$ of ROH[16] leaving group, at 30 °C and $\mu = 0.2$. The apparent second-order rate constant for reaction of each ROOH with (3)$Fe^{III}(H_2O)(OH)$ was obtained from the intercept of a buffer dilution plot (*vide supra*). The reactions of percarboxylic acids with (3)$Fe^{III}(H_2O)_2$ occur in the stopped-flow time range and are subject to inhibition by increasing acetate concentration. The rates of reactions of peracids with (3)$Fe^{III}(H_2O)_2$ are first order in porphyrin concentration and essentially unaffected by proton activity between pH 2.0 and 6.8. Control reactions with peracids in the presence of ABTS, where the porphyrin was omitted, revealed that the rate of appearance of $ABTS^{\bullet+}$ is at least 60-fold faster in the presence of $1.9 \times 10^{-6}$ M (3)$Fe^{III}(H_2O)(OH)$. A detectable break in the plot of log $k_{ly}$ vs p$K_a$ (ROH) is seen at p$K_a \sim 6$ (Figure 5). At p$K_a < 6$, the slope of the plot is −1.0, while at p$K_a > 6$, the slope is −0.2. Thus, sensitivity of percarboxylic acid decomposition to electronic effects in R is pronounced, while reactions of alkyl ROOH and $H_2O_2$ are only modestly affected by changes in p$K_a$(ROH).

## Discussion

The thermodynamics, kinetics, and product distributions for the reaction of structurally homologous, but oppositely charged, multianionic (1)$Fe^{III}(X)_2$ and (2)$Fe^{III}(X)_2$, and multicationic (3)-$Fe^{III}(X)_2$ (Chart 1, X = $H_2O$ and/or $HO^-$) with alkyl and acyl hydroperoxides have been studied. To the best of our knowledge, (3)$Fe^{III}(X)_2$ is one of only two cationic porphyrins which are monomeric and well behaved in aqueous solution over a wide range of pH and porphyrin concentrations.[17] The previously studied (1)$Fe^{III}(X)_2$ and (2)$Fe^{III}(X)_2$ are the only known water soluble, multianionic, and non-μ-oxo dimer forming iron-(III) porphyrins.

**The reactions of *t*-BuOOH ($6.0 \times 10^{-5}$ M) with (3)$Fe^{III}(X)_2$ ($1 \times 10^{-7}$–$5.4 \times 10^{-6}$ M)** were examined at 30 °C under conditions of ionic strength between 0.075 and 0.75 M, between pH 0.9 and 12.1. The reactions are first-order in both $[t\text{-BuOOH}]_i$ and $[(3)Fe^{III}(X)_2]$. A feature indigenous to the polycationic (3)$Fe^{III}(X)_2$ is the inhibition of its reaction with *t*-BuOOH due to ligation by oxyanion buffers. This is not observed with the tetraanionic (1)$Fe^{III}(X)_2$. The influence of buffer ligation on rate constants was corrected for by extrapolation of plots of observed first-order rates vs total buffer concentration (Figure 3) to zero buffer concentration. The pseudo-first-order rate constants at zero buffer concentration for the reaction at a given $[(3)Fe^{III}(X)_2]$ and pH are abbreviated as $k_{obsd}$; the pH-dependent second order rate constants of $k_{obsd}/[(3)Fe^{III}(X)_2]$ are referred to as $k_{ly}$. A previous study by Lindsay Smith and Lower, using tetracationic *meso*-5,10,15,20-tetrakis-(*N*-methyl pyridyl)porphinatoiron(III) chloride (**TMPyP**)$Fe^{III}(X)_2$ to catalyze the decomposition of *t*-BuOOH, revealed that the nature of the buffer species influences the rate constants.[18] Unlike amine bases, which upon monoligation to an iron(III) tetraphenylporphyrin cause substantial enhancements of the rates of reactions with ROOH species,[6i] carboxylate anion monoligation to (3)$Fe^{III}(X)_2$ (see previous paper in this issue) causes some small amount of inhibition of reaction. The decrease in the rate of the reaction of (3)$Fe^{III}(X)_2$ with *t*-BuOOH going from zero buffer concentration to 0.1 M acetate buffer at pH 5.45 is 2-fold (Figure 3). A rationale for the buffer inhibition could be that the reacting complex **PH** (Scheme 4) at zero buffer concentration (I in Chart 2) is replaced by a monoligated acetate complex (**II** in Chart 2) in acetate buffer. Neither complex in Chart 2 carries a formal charge (recall that the porphyrin is a dianionic ligand). Two kinetically equivalent representations

(16) p$K_a$ values for carboxylic acids are obtained from the literature, whereas alcohol p$K_a$'s were calculated from an equation relating the p$K_a$ of a trisubstituted methanol (RR'R''COH) to the $\sigma_I$ values of the substituents. The p$K_a$ for methanol (R = R' = R'' = H) is 15.5: Ballinger, P.; Long, F. A. *J. Am. Chem. Soc.* **1960**, *82*, 792. $\sigma_I$ parameters were taken from: Charton, M. *J. Org. Chem.* **1964**, *29*, 1222. $\rho_I$ for plots of p$K_a$ vs $\Sigma\sigma_I$ of RR'R''COH are between −8.2 and −8.4: Fox, J. P.; Jencks, W. P. *J. Am. Chem. Soc.* **1974**, *96*, 1436.

(17) Miskelly et al. found *meso*-αβαβ-tetrakis((*o*-(*N*-methylnicotinamido)phenyl)porphyrinatoiron(III) bromide {(αβαβ-**TMNP**)$Fe^{III}$(Br)} to be resistant to μ-oxo dimer formation in water: Miskelly, G. M.; Webley, W. S.; Clark, C. S.; Buckingham, D. A. *Inorg. Chem.* **1988**, *27*, 3773. See Chart 2 in the previous paper in this issue for the structure.

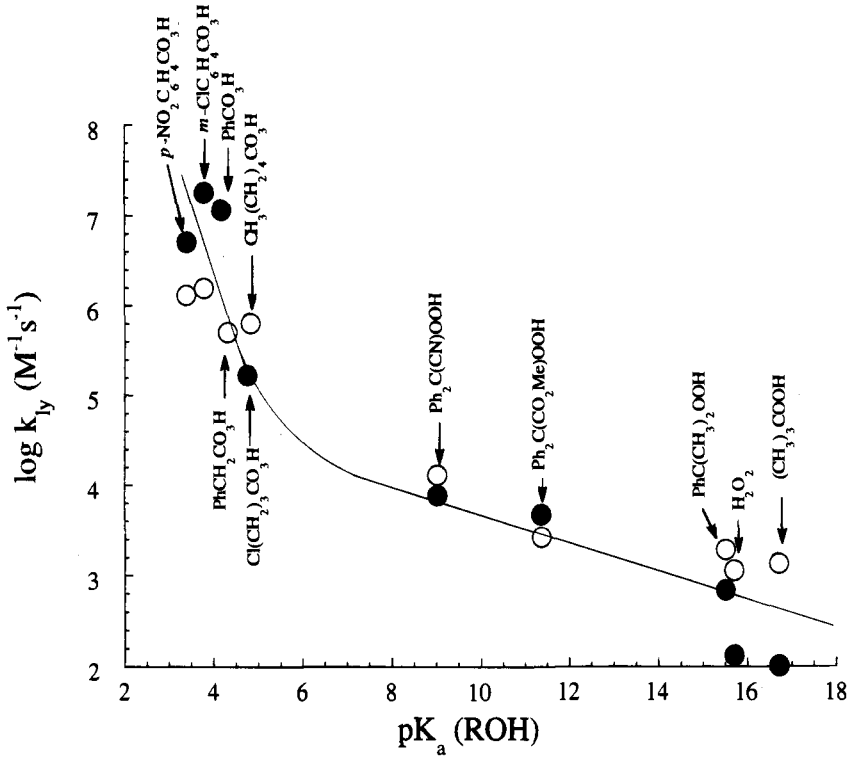


**Figure 5.** Plot of the logarithm of second order rate constants, $k_{ly}$ ($M^{-1}$ $s^{-1}$), for reactions of (**3**)$Fe^{III}(X)_2(O)$ with alkyl and acyl hydroperoxides vs p$K_a$ of leaving groups (alcohols or carboxylic acids[16]) at pH 5.2, 30 °C, and $\mu = 0.2$. Initial peroxide concentrations, $[ROOH]_i$, were $6.0 \times 10^{-5}$ M, while porphyrin concentration was generally $7.7 \times 10^{-7}$–$1.9 \times 10^{-6}$ M. Each lyate rate was obtained from a buffer dilution experiment in acetate buffer, as detailed in the legend to Figure 3. {For comparison are included log $k_{ly}$ values (●) for (**1**)$Fe^{III}(X)_2$ at pH 6.7; ref 6a.}

**Chart 2**

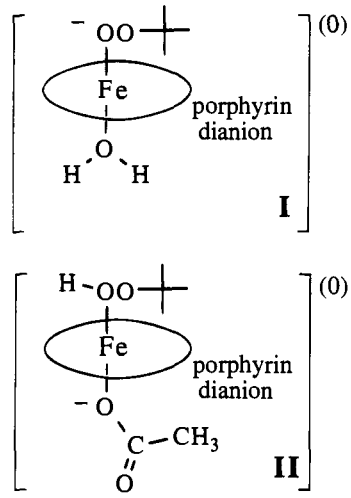


of I can be formulated (**PH** in Scheme 4), while II requires that the acetate ligand be protonated. Buffer inhibition can be explained by the breakdown of I proceeding at a greater rate compared to II.

The pH-rate profiles for the reactions of iron(III) tetraphenylporphyrins with *t*-BuOOH, obtained from plots of log $k_{ly}$ vs pH reveal that the rate constants are not greatly different from octacationic (**3**)$Fe^{III}(X)_2$ and tetraanionic (**1**)$Fe^{III}(X)_2$ (Table 2). Shifting of the profile for (**3**)$Fe^{III}(X)_2$ in Figure 4 has occurred, such that the pH optimum in the intermediate range for (**3**)-$Fe^{III}(X)_2$ in Figure 4 has occurred, such that the pH optimum in the intermediate range for (**3**)$Fe^{III}(X)_2$ (at pH 5.4 in Figure 4) is found to be at a lower pH than in the reactions of (**1**)-$Fe^{III}(X)_2$ (pH 6.7).[6d] This is in accord with the lowering of the p$K_a$ value of the ligated water molecule on (**3**)$Fe^{III}(H_2O)_2$ compared with that of (**1**)$Fe^{III}(H_2O)_2$ (5.8 and 6.7, respectively at $\mu = 0.2$). With (**3**)$Fe^{III}(X)_2$, the effect of increased ionic strength, at a constant 0.1 M total buffer concentration, is to modestly increase reaction rates (Table 1). The largest rate enhancements occur at intermediate pH corresponding to the middle bell-shaped curve of the pH-rate profile of Figure 4, where **PH** (Scheme 4) is the productive intermediate. The dependence of $k_{ly}$ on ionic strength at intermediate pH parallels competitive inhibition by buffer anions. At high ionic strength, buffer ligation is likely impeded, which provides rationale for the increases in $k_{ly}$ in 0.1 M buffers at pH 6.1 (6.4-fold with cacodylate) and 6.7 (4.8-fold with phosphate) with increased ionic strength.

The change from octacationic (**3**)$Fe^{III}(X)_2$ to tetraanionic (**1**)-$Fe^{III}(X)_2$ brings about a change in the second order rate constant $\{k_1k_2/(k_2 + k_{-1})\}$ of 3.5-fold in favor of (**3**)$Fe^{III}(X)_2$ (Table 2). In this pH region, $k_2$ is reasonably assigned as the rate determining step for the forward reaction of $PH_2^+$ (Scheme 3).[6d] If this is so, the 3-fold difference in rate may be due to changes in the equilibrium constant for peroxide ligation ($k_1/k_{-1}$) or the breakdown of the complex ($k_2$). Thus, it is possible that the increase in $k_2$ is larger than 3.5-fold. Consider also the composite kinetic term $k_6k_5K_D/(k_6 + k_{-5})$ in Table 2 and Scheme 3, for which the decrease is 70-fold relative to the same term for (**1**)$Fe^{III}(X)_2$. A likely explanation for at least a portion of the rate differential is the stronger affinity of (**3**)$Fe^{III}(X)_2$ for $HO^-$, reflected in a smaller $K_D$. In our study of acetate ion ligation to (**3**)$Fe^{III}(H_2O)_2$ (previous paper in this issue) we showed that the cationic porphyrin attracts anions which ligate to the central iron(III), a feature not shared by tetraanionic (**1**)$Fe^{III}(X)_2$.

**Linear free energy relationship of the log of the second order rate constant extrapolated to zero buffer concentration ($k_{ly}$) vs p$K_a$ ROH** for the reactions of ROOH with metalloporphyrins have been employed to elucidate the dependence of rate constants upon electronic effects in the ROH moieties. A break in the plot of log $k_{ly}$ for various ROOH vs p$K_a$(ROH) (Figure

**Scheme 5**

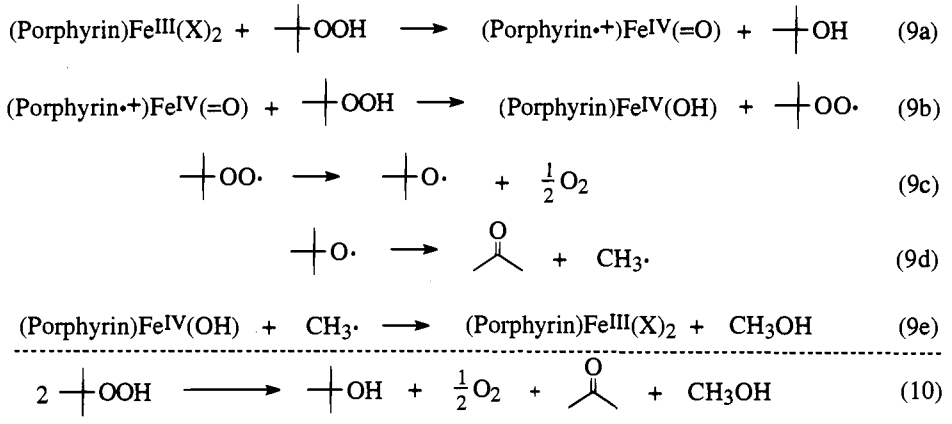


5) at p$K_a$ ~ 6 from high sensitivity for acidic ROH to modest sensitivity to p$K_a$(ROH) for weakly acidic ROH is seen. We have previously observed breaks in the plots of log $k_{ly}$ vs p$K_a$(ROH) for reactions of ROOH with (**1**)Fe$^{III}$(X)$_2$[6a] {included as the dashed line in Figure 5}. The phenomenon is also apparent with cobalt(II) porphyrins[4f] and iron(III) porphyrins[4g] in non-aqueous solutions. A break is observed with Mn$^{III}$ porphyrins[4c,d] at high p$K_a$ of ROH and no break is seen with (TPP)Cr$^{III}$ species[4h] or EDTA-Fe$^{III}$.[4j]

The two different slopes of the plot of Figure 5 are −1.0 for the reactions of $RCO_3H$ and (**3**)Fe$^{III}$(X)$_2$ and −0.2 for the reactions of alkyl-OOH and $H_2O_2$. We have proposed in previous studies that the break in the plot of log $k_{ly}$ vs p$K_a$(ROH) indicates a change of mechanism from 2e$^-$ transfer and heterolytic O–O bond breaking with $RCO_3H$ and acidic hydroperoxides to rate determining 1e$^-$ transfer and homolytic O–O bond scission for the less reactive alkyl hydroperoxides.[6a,c,d,h] The lack of general catalysis (acid or base) in the O–O cleavage reactions of acyl and alkyl hydroperoxides with (**3**)Fe$^{III}$(X)$_2$ as well as in the reactions with (**1**)Fe$^{III}$(X)$_2$[6a] negates arguments based upon the use of More O'Ferrall–Jencks[7] (or MAR[8]) diagrams to explain the apparent break in the plots of log $k_{ly}$ vs p$K_a$(ROH).

Rate determining homolysis of RO–OH if followed by rapid second-electron transfer provides a transition state characteristic of homolysis and products consistent with heterolytic cleavage (Scheme 1). An alternative explanation for the break in the plot of log $k_{ly}$ vs p$K_a$ of ROH is that the mechanism is heterolytic, but that the degree to which the O–O bond is broken in the rate-limiting transition state is altered as p$K_a$(ROH) changes. According to the Hammond postulate, the most exothermic reactions (those involving $RCO_3H$) would have early transition states with very little O–O bond breaking and, thus, should not be very sensitive to electronic factors in $RCO_2^-$ leaving group (small $\beta_{lg}$). Conversely, the least exothermic reactions (those with *t*-BuOOH and $H_2O_2$) should display advanced O–O bond breaking in the late transition states and hence be more sensitive to stabilization of the forming $RO^-$ entities (larger $\beta_{lg}$). Inspection of Figure 5 shows that the opposite is true, and therefore the proposal is in violation of the Hammond postulate.

**The identities of the products of the reactions of (3)Fe$^{III}$(X)$_2$ with *t*-BuOOH** reveal the radical nature of the O–O bond scission step. Consider the reactions which were carried out in the presence of ABTS (entries labeled with + in Table 3). Hypervalent porphyrin species {(**3**)Fe$^{IV}$(X)$_2$ or (**3**$^{\bullet+}$)Fe$^{IV}$(X)$_2$} and radical products, such as $(CH_3)_3CO^{\bullet}$ in the event of homolytic cleavage of $(CH_3)_3COOH$, are being trapped by ABTS. Regardless of the nature of the O–O bond breaking step, 100% *t*-BuOH is anticipated in the presence of ABTS. Inspection of Table 3 shows that this is not the case, and small amounts of acetone are invariably formed. When the trapping agent is omitted, the product ratios of acetone and *t*-BuOH are essentially reversed. In this case, yields of *t*-BuOH less than 50% are observed (43, 15, and 17%), with acetone as the main product at all pH values. The product yields and A/B ratios in Table 3 in the absence of ABTS can be discussed in terms of four mechanistic proposals: (a) heterolysis of *t*-BuOOH with a contribution from radical chain reactions; (b) a radical chain mechanism initiated by (**3**)Fe$^{IV}$(X)(O); (c) Fenton chemistry involving (**3**)Fe$^{II}$ and (**3**)Fe$^{III}$ states; or (d) homolysis of *t*-BuOOH. An evaluation of the four mechanistic possibilities in (a)–(d) follows.

(a) Heterolytic scission of *t*-BuOOH requires that the yield of *t*-BuOH from the reaction with (**3**)Fe$^{III}$(X)$_2$ exceed 50%. In the first reaction of Scheme 5, compound I and *t*-BuOH are produced in an overall heterolytic oxidation of iron(III) porphyrin by *t*-BuOOH. In the following step *t*-BuOH and *t*-BuOOH will compete as substrates for (porph$^{\bullet+}$)Fe$^{IV}$(=O). The oxidation of *t*-BuOOH to provide *t*-BuOO$^{\bullet}$ is favored (eq 9b) by many kcal/mol over the oxidation of *t*-BuOH to yield *t*-BuO$^{\bullet}$.[11b] Under the ideal conditions of low catalyst concentrations and ~10-fold excess of *t*-BuOOH over catalyst, *t*-BuOH will be formed in 50% yield if the mechanism involves heterolytic cleavage of the hydroperoxide O–O bond. At pH 5.6 and 9.3 the percentages of *t*-BuOH product in the absence of ABTS are but 15% and 17%, respectively. At these values of pH, the mechanism cannot be that of Scheme 5. According to Table 3, the largest proportion of *t*-BuOH obtained in the absence of ABTS is 43 (±4)% at pH 2.0. On the basis of the percentage yield of *t*-BuOH one cannot rule out a contribution of heterolytic scission (Scheme 5) or radical combination to provide the increased yield of *t*-BuOH at low pH. We observe, however, that the ratios of acetone to *t*-BuOH yields in the absence of ABTS are always greater than 1.3 (Table 3), hence a heterolytic mechanism cannot dominate at any pH.

Epoxidation of alkenes with retention of stereochemistry by the species produced in the reaction of an iron(III) porphyrin and ROOH species is taken to establish the formation of the hypervalent (porphyrin$^{\bullet+}$)Fe$^{IV}$(X)$_2$.[10] Alkene epoxidations are generally studied in organic solvents using very high concentrations of substrate and hydroperoxide. Details of reactions under such conditions are difficult to elucidate and remain obscure. *trans*-Stilbene oxide is the major product from reaction of *cis*-stilbene with *t*-BuOOH in the presence of iron(III) tetraarylporphyrins.[6k,j] Labeque and Marnett have shown that nonstereospecific epoxidations of alkenes such as *cis*-stilbene occur in the presence of alkyl-OO$^{\bullet}$.[19] A mere 3% of stereospe-

**Scheme 6**

$$(\text{porph})\text{Fe}^{\text{III}}(\text{X})_2 + t\text{-BuOOH} \rightarrow \|(\text{porph})\text{Fe}^{\text{IV}}(\text{X})(\text{OH}) + t\text{-BuO}^{\bullet}\| \quad (11a)$$

$$\|(\text{porph})\text{Fe}^{\text{IV}}(\text{X})(\text{OH}) + t\text{-BuO}^{\bullet}\| \rightarrow (\text{porph})\text{Fe}^{\text{IV}}(\text{X})(\text{OH}) + t\text{-BuO}^{\bullet} \quad (11b)$$

$$2t\text{-BuO}^{\bullet} \rightarrow (t\text{-BuO})_2 \quad (11c)$$

$$2t\text{-BuOO}^{\bullet} \rightarrow (t\text{-BuOO})_2 \rightarrow (t\text{-BuO})_2 + \text{O}_2 \quad (11d)$$

$$t\text{-BuO}^{\bullet} + t\text{-BuOOH} \rightarrow t\text{-BuOH} + t\text{-BuOO}^{\bullet} \quad (11e)$$

$$t\text{-BuOO}^{\bullet} \rightarrow t\text{-BuO}^{\bullet} + {}^1/_2\text{O}_2 \quad (11f)$$

**Scheme 7**

$$(\text{Porphyrin})\text{Fe}^{\text{III}}(\text{X})_2 + \text{—OOH} \longrightarrow (\text{Porphyrin})\text{Fe}^{\text{II}}(\text{X})_2 + \text{H}^+ + \text{—OO}^{\bullet} \quad (12a)$$

$$\text{—OO}^{\bullet} \longrightarrow \text{—O}^{\bullet} + \tfrac{1}{2}\text{O}_2 \quad (12b)$$

$$\text{—O}^{\bullet} \longrightarrow \text{O=C(CH}_3\text{)}_2 + \text{CH}_3^{\bullet} \quad (12c)$$

$$(\text{Porphyrin})\text{Fe}^{\text{III}}(\text{X})(\text{OH}) + \text{CH}_3^{\bullet} \xrightarrow{\text{H}_2\text{O}} (\text{Porphyrin})\text{Fe}^{\text{II}}(\text{X})_2 + \text{CH}_3\text{OH} \quad (12d)$$

$$2(\text{Porphyrin})\text{Fe}^{\text{III}}(\text{X})_2 + 2\text{—OOH} \longrightarrow 2(\text{Porphyrin})\text{Fe}^{\text{II}}(\text{X})_2 + \tfrac{1}{2}\text{O}_2 + \text{O=C(CH}_3\text{)}_2 + \text{CH}_3\text{OH} \quad (13)$$

cific epoxidation of the highly efficient radical probe (Z)-1,2-bis(*trans*-2,*trans*-3-diphenylcyclopropyl)ethene (**Z**)[6o] was observed in the presence of tetrakis(2,6-dichlorophenylporphinatoiron(III) and *t*-BuOOH, the remainder products of radical

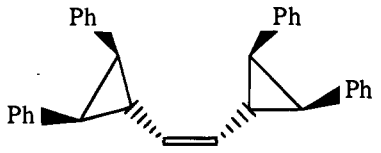


(**Z**)

trapping.[6k] No epoxidation of the water soluble 3-cyclohexene 1-carboxylate has been observed in aqueous solution with *t*-BuOOH and (**1**)$Fe^{III}(X)_2$ or (**2**)$Fe^{III}(X)_2$.[6a,f]

(b) A radical chain mechanism cannot account for the high yields of acetone and methanol in our reactions. Features of such a mechanism are outlined in Scheme 6. Initiation (eq 11a) occurs from *t*-BuOOH homolysis to give *t*-$BuO^{\bullet}$, which becomes an uncaged radical in eq 11b. The sequence of eqs 11c–f should be important in an ensuing radical chain propagation. Our studies of the products of *t*-BuOOH decomposition in aqueous solution, herein and elsewhere,[6b] do not support di-*tert*-butyl peroxide as a major product from *t*-BuOOH decomposition by iron(III) porphyrin in water, and eqs 11c and 11d cannot be important reactions. The concentration of *t*-$BuOO^{\bullet}$ is controlled by the porphyrin concentration, the latter being on the order of $10^{-6}$ M. At this low concentration of catalyst, the bimolecular reaction of eq 11d is expected to be slow ($k_{obsd} \sim 10^3\ s^{-1}$)[20] compared with the unimolecular fragmentation of *t*-$BuO^{\bullet}$ (eq 9d, $k_1 = 1.4 \times 10^6\ s^{-1}$).[21] Since oxygen has not been observed as a product from the reactions of (**1**)$Fe^{III}(X)_2$ with *t*-BuOOH,[6b] eqs 11d–f are judged unimportant. The products from the reactions of *t*-BuOOH with (**TMPyP**)$Fe^{III}(X)_2$ at pH 9.3 were analyzed in detail by Lindsay Smith and Lower,[18] who found that acetone was the main product in the presence of ABTS. Minute amounts of *t*-BuOH were found as well as traces of methane and ethane. Also, substantial amounts of formaldehyde, methyl-*tert*-butyl peroxide, and methanol were produced in the absence of ABTS. Consequently, the radical chain mechanism of Scheme 6 is not operational and cannot be used to explain the product yields observed herein, in our previous studies,[6b,h] as well as product yields obtained by other workers.[18]

(c) "Fenton chemistry" involving iron(III) and iron(II) porphyrins (Scheme 7) has previously been considered as a kinetically competent alternative to a homolytic cleavage mechanism {as in (d), *vide infra*}.[6c] According to the balance of eq 13 in Scheme 7, *t*-BuOH should not be a product of this sequence of reactions. All *t*-BuOOH equivalents are converted to uncaged *t*-$BuOO^{\bullet}$ and *t*-$BuO^{\bullet}$ radicals in Scheme 7. The radicals will undergo facile cleavage (eq 12b, second order rate constant of $1 \times 10^9\ M^{-1}\ s^{-1}$)[22] and/or fragmentation (eq 12c, unimolecular rate constant $1.4 \times 10^6\ s^{-1}$)[21] in aqueous solution. The scheme indicates that iron(II) species will accumulate (eq 13), unless $O_2$ reacts with two (porphyrin)$Fe^{II}$ species to generate (porphyrin)$Fe^{IV}O$ (eq 14).[23] We do observe this to be so,

$$2(\text{porph})\text{Fe}^{\text{II}} + \text{O}_2 \rightarrow (\text{porph})\text{Fe}^{\text{III}}\text{OOFe}^{\text{III}}(\text{porph}) \rightarrow 2(\text{porph})\text{Fe}^{\text{IV}}\text{O} \quad (14)$$

however the observation of *t*-BuOH as a product in the absence and presence of ABTS argues against a radical chain mechanism, such as that in Scheme 7. The relatively small percentage of (porphyrin)$Fe^{II}$ trapped in the reactions of (**1**)$Fe^{III}(X)_2$ {10% trapping as (**1**)$Fe^{II}(X)(CO)$ adduct}[6c] and (**2**)$Fe^{III}(X)_2$ {20%

(18) Lindsay Smith, J. R.; Lower, R. J. *J. Chem. Soc. Perkin Trans. 2* **1991**, 31.

(19) (a) Labeque, R.; Mamett, L. J. *J. Am. Chem. Soc.* **1987**, *109*, 2828. (b) Labeque, R.; Marnett, L. J. *Biochemistry* **1988**, *27*, 7060. (c) Labeque, R.; Marnett, L. J. *J. Am. Chem. Soc.* **1989**, *111*, 6621.

(20) In a back of an envelope calculation, multiplying the known rate of dimerization of *t*-$BuO^{\bullet}$ (ref 22) and the porphyrin concentration ($1 \times 10^{-6}$ M) gives the pseudo-first-order rate constant.

(21) Erben-Russ, M.; Michael, C.; Bors, W.; Saran, M. *J. Phys. Chem.* **1987**, *91*, 2362.

(22) Niki, E.; Kamiya, Y. *J. Am. Chem. Soc.* **1974**, *96*, 2129.

(23) (a) Chin, D.-H.; Gaudio, J. D.; La Mar, G. N.; Balch, A. L. *J. Am. Chem. Soc.* **1977**, *99*, 5486. (b) Balch, A. L.; Chan, Y.-W.; Cheng, R. J.; La Mar, G. N.; Latos-Grazynski, L.; Renner, M. W. *J. Am. Chem. Soc.* **1984**, *106*, 7779.

trapping as (**2**)$Fe^{II}(X)(CO)$}[6f] with alkyl hydroperoxides also cannot be explained by predominant Fenton chemistry, since the rate of trapping of $Fe^{II}$ porphyrins by CO is known to be very rapid ($>10^6$ $M^{-1}$ $s^{-1}$).[24] If Fenton chemistry were the major contributing mechanism, most of the porphyrin should be trapped as the ferrous species with CO upon completion of one turnover.

(d) Homolytic cleavage of alkyl ROO(H) to yield an iron(IV) porphyrin and RO$^\bullet$ (Scheme 8) best explains our present

**Scheme 8**

**Association:**

$$(porph)Fe^{III}(X)_2 + (CH_3)_3COOH \rightarrow \|(porph)Fe^{IV}(X)(OH) + (CH_3)_3CO^\bullet\| \quad (15a)$$

**Caged reactions:**

$$\{\|(porph)Fe^{IV}(X)(OH) + (CH_3)_3CO^\bullet\| \rightarrow \|(porph^{\bullet+})Fe^{IV}(X)(O) + (CH_3)_3COH\|\} \quad (15b)$$

$$\|(porph)Fe^{IV}(X)(OH) + (CH_3)_3CO^\bullet\| \rightarrow \|(porph)Fe^{IV}(X)(OH) + (CH_3)_2CO + CH_3^\bullet\| \quad (15c)$$

$$\|(porph)Fe^{IV}(X)(OH) + CH_3^\bullet\| + H_2O \rightarrow \|(porph)Fe^{III}(X)(H_2O) + CH_3OH\| \quad (15d)$$

**Uncaged reactions:**

$$\{(porph^{\bullet+})Fe^{IV}(X)(O) + (porph)Fe^{III}(X)_2 \rightarrow 2(porph)Fe^{IV}(X)(OH)\} \quad (15e)$$

$$(CH_3)_3CO^\bullet \rightarrow (CH_3)_2CO + CH_3^\bullet \quad (15f)$$

$$(porph)Fe^{IV}(X)(OH) + CH_3^\bullet + H_2O \rightarrow (porph)Fe^{III}(X)(H_2O) + CH_3OH \quad (15g)$$

**Further reactions:**

$$(porph)Fe^{III}(X)(OH) + CH_3^\bullet + H_2O \rightarrow (porph)Fe^{II}(X)(H_2O) + CH_3OH \quad (15h)$$

$$2(porph)Fe^{II}(X)(H_2O) + O_2 \rightarrow (porph)(X)Fe^{III}O\text{-}OFe^{III}(X)(porph) \quad (15i)$$

$$(porph)(X)Fe^{III}O{-}OFe^{III}(X)(porph) \rightarrow 2(porph)Fe^{IV}(X)(O) \quad (15j)$$

$$(porph)Fe^{IV}(X)(O) + (porph)Fe^{II}(X)(H_2O) \rightarrow 2(porph)Fe^{III}(X)(OH) \quad (15k)$$

**Peroxide oxidation:**

$$(porph)Fe^{IV}(X)(O) + (CH_3)_3COOH \rightarrow (porph)Fe^{III}(X)(OH) + (CH_3)_3COO^\bullet \quad (15l)$$

$$(CH_3)_3COO^\bullet \rightarrow {}^1/_2O_2 + (CH_3)_3CO^\bullet \rightarrow (CH_3)_2CO + CH_3^\bullet \quad (15m)$$

$$\{(CH_3)_3COO^\bullet + CH_3^\bullet \rightarrow (CH_3)_3O{-}OCH_3\} \quad (15n)$$

as well as previous results from studies of the reactions of water soluble iron(III) porphyrins with *t*-BuOOH in low turnover {to avoid radical chain processes} experiments. The low yield of $(CH_3)_3COH$ product obtained in the absence of ABTS presumably reflects the propensity of untrappable $(CH_3)_3CO^\bullet$ {i.e., ||(**3**)$Fe^{IV}(OH)$ $(CH_3)_3CO^\bullet$||} to undergo reduction by transfer of a second electron from the porphyrin in the "caged" reaction with the metalloporphyrin (eq 15b). Any (porph$^{\bullet+}$)$Fe^{IV}(X)(O)$ formed in such a trapping event will likely comproportionate with another Fe(III) species (eq 15e). Methanol presumably results from trapping of methyl radicals resulting from cleavage of *t*-BuO$^\bullet$ (eqs 15c, d, f, and h). Acetone and methanol should be produced in equal amounts if the hypervalent iron(IV) porphyrin species (porph)$Fe^{IV}(X)(OH)$ faithfully delivers HO$^\bullet$ to the incipient methyl radical in a "rebound" mechanism (eq 15d). However, our previous work[6b] and that of Lindsay Smith and Lower[18] has established formaldehyde as a product of *t*-BuOOH cleavage catalyzed by iron(III) porphyrins in the presence of oxygen. This can be explained by $O_2$ oxidation of $CH_3^\bullet$.[18] In the present case, the sum of the yields of acetone and *t*-BuOH serves to account for the majority of the mass balance in Table 3, both in the presence and absence of ABTS. Scheme 8 accounts for the observed products of the reactions, and the fraction of untrappable $(CH_3)_3CO^\bullet$. In the absence of ABTS, most of $(CH_3)_3CO^\bullet$ undergoes fragmentation. When ABTS is present, most of the radical is trapped. Even in the presence of a very large excess of ABTS,[6b] a fraction slightly larger than 10% will invariably undergo facile fragmentation "in the cage" (eq 15c). This, again, is a strong indication that a certain amount of $(CH_3)_3CO^\bullet$ is untrappable due to competing cage reactions. The observation of (porphyrin)$Fe^{II}$ species can be rationalized by the reaction of methyl radical with (porphyrin)$Fe^{III}(X)(OH)$ (eq 15h, rate constant = $2.3 \times 10^9$ $M^{-1}$ $s^{-1}$).[25]

In addition to *t*-BuOOH, cumyl hydroperoxide {$PhC(CH_3)_2$-OOH} and diphenyl carbomethoxymethyl hydroperoxide {$Ph_2C$-$(CO_2Me)$OOH} have previously been shown to give products consistent with radical cleavage of the O–O bonds upon reaction with (**1**)$Fe^{III}(X)_2$.[6h] In summary, a *homolytic cleavage of the O–O bond of t-BuOOH catalyzed by the water soluble iron(III) porphyrins (Scheme 8), is the only mechanistic scheme capable of explaining the observed products and their yields.*

**Is Homolytic Cleavage of the O–O Bonds an Important Feature in the Mechanisms of Reactions of Alkyl Hydroperoxides with Heme-Bound Iron(III)?** Two recent examples indicate that homolysis, although observable, is an underrated mechanistic contribution in ROOH cleavage reactions catalyzed by heme proteins. Ortiz de Montellano and co-workers recently reported on the use of 4-hydroperoxy-4-methyl-2,6-di-*tert*-butylcyclohexa-2,5-dien-1-one (BHTOOH) as a reporter peroxide for homolytic cleavage in reactions with myoglobins.[26]

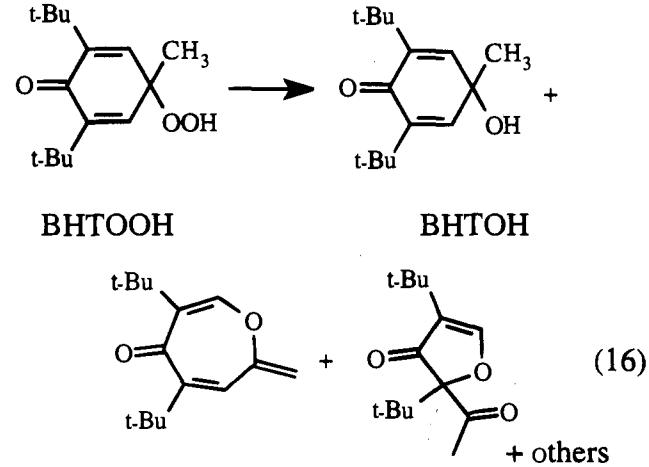


(16)

Relatively large proportions (27–39%) of rearrangement products (eq 16) are consistent with homolysis of the O–O bond of

(24) Geibel, J.; Cannon, J.; Cambell, D.; Traylor, T. G. *J. Am. Chem. Soc.* **1978**, *100*, 3575.

(25) Brault, D.; Neta, P. *J. Am. Chem. Soc.* **1981**, *103*, 2705.

(26) Allentoff, A. J.; Bolton, J. L.; Wilks, A.; Thompson, J. A.; Ortiz de Montellano, P. R. *J. Am. Chem. Soc.* **1992**, *114*, 9745.

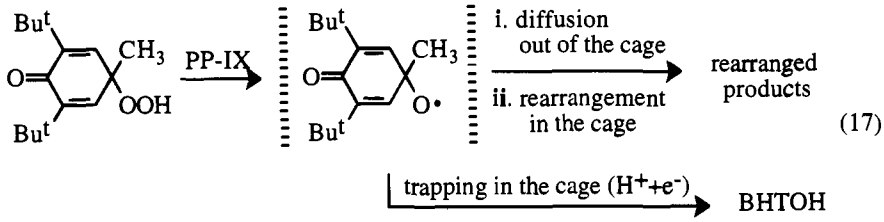


(17)

BHTOOH (eq 17). The remaining unrearranged alcohol BHTOH was postulated to arise from heterolysis of BHTOOH. An alternative and equally plausible interpretation is to consider the peroxide scission as predominantly homolytic but allowing for competing "trapping" of the BHTO• radical by a second electron from the prophyrin (eq 17).

Adachi et al. studied mutants of myoglobins where the axial ligand HIS 93 (F8) was exchanged for CYS and TYR, in order to emulate the iron complexes of cytochrome P-450 and catalase, respectively.[27] The importance of the proximal ligand in bringing about homolytic or heterolytic O−O bond cleavage was assessed by use of cumyl hydroperoxide {$PhC(CH_3)_2OOH$}. The yield of acetophenone, derived from fragmentation of the $PhC(CH_3)_2O^•$ radical produced by homolysis of the O−O bond, was taken as a measure of the radical character of peroxide scission. The percentages of acetophenone were found to be 24, 12, and 25% for the wild type, HIS93CYS and HIS93TYR enzymes, respectively. The HIS93CYS mutant displayed a marked enhancement of the peroxide cleavage rate. The electron rich thiolate can be (i) affecting the the nature of the O−O bond scission, shifting the mechanism toward heterolytic, and/or (ii) increasing the rate of trapping by electron transfer to $PhC(CH_3)_2O^•$ in the cage due to $-S^-$ ligation to putative (porphyrin$^{•+}$)$Fe^{IV}$(O) intermediate.

In relation to the two studies on myoglobin catalyzed hydroperoxide cleavage, it is easy to visualize how a myoglobin active site achieves more effective caging of a radical in the protein interior than is possible with a synthetic iron(III) porphyrin, where the substrate is directly exposed to the aqueous environment during catalysis. Further, protoporphyrin-IX iron(III) porphyrins are more electron rich than (TPP)$Fe^{III}$(X) derivatives (the latter have *meso*-phenyl rings as inductively electron withdrawing groups and lack the electron donating alkyl substituents on the $\beta$-positions of protoporphyrin IX). A (protoporphyrin-IX$^{•+}$)$Fe^{IV}$(OH) species is therefore likely to posess a more negative reduction potential than a representative (TPP$^{•+}$)$Fe^{IV}$(OH) species. The reduction of the initially produced RO• radical by (protoporphyrin-IX)$Fe^{IV}$(OH) to give the net two-electron transfer reaction should thus be more facile than with a (TPP)$Fe^{IV}$(OH). Regardless of the interpretation, it should be obvious that homolytic cleavage is a contributing mechanism in the reaction of protoporphyrin-IX iron containing proteins with peroxide substrates. Parenthetically, the observed second order rate constants for the reactions of the alkyl hydroperoxides with myoglobins[26,27] are similar in magnitude to those obtained in our model studies in water ($\sim 10^2\ M^{-1}\ s^{-1}$).

## Conclusions

Comparison of the rate constants at varying pH for the reaction of *t*-BuOOH with multicationic (**3**)$Fe^{III}(X)_2$ and multianionic (**1**)$Fe^{III}(X)_2$ in aqueous solution reveals that the charge surrounding the iron(III) does not greatly influence the reaction. Also, the rate limiting O−O scission step is radical in nature and is best described by a homolytic cleavage of RO−OH. Heterolytic cleavage must produce *t*-BuOH in 50% yield because in a heterolytic mechanism there is a competition of *t*-BuOH and *t*-BuOOH for the (porphyrin$^{•+}$)$Fe^{IV}$(O) oxidant, and the winnder is invariably the more easily oxidized *t*-BuOOH. Such high yields of *t*-BuOH are not observed, and the mechanism cannot involve heterolysis. There has been an insistence by some that our inability to observe general-acid catalysis was due to electrostatic shielding by the negative charges of tetraanionic (**1**)$Fe^{III}(X)_2$ and (**2**)$Fe^{III}(X)_2$. This cannot be the case, for we now find no general-acid or general-base catalysis with the octacationic (**3**)$Fe^{III}(X)_2$. An explanation for the lack of linearity in plots of log of the second order rate constants (at given pH values) vs the $pK_a$ of the leaving ROH {as seen in Figure 5} has been offered by Perrin, Traylor, and co-workers.[28] Their explanation is based upon the use of More O'Ferrall−Jencks[7] (or MAR[8]) energy surfaces and explicitly requires that the reaction of [(porph)$Fe^{III}$]$^+$ salts with $RCO_3H$ and R−OOH is driven by general-acid catalysis. The concertedness of heterolytic O−O bond cleavage and general acid proton transfer is proposed to be dependent upon the proton basicity of the leaving $RCO_2^-$ and ROH {changing transition state structure}. This explanation is of questionable value since it is not applicable to the nonlinear plots of log $k_{rate}$ vs $pK_a$ of ROH observed in water where general-acid catalysis is not observed (this study and ref 6a,c,d,h).

**Acknowledgment.** Ö.A. thanks the American-Scandinavian Foundation for partial financial support in the form of fellowships. The study was supported by the National Institutes of Health.

JA9416302

(27) Adachi, S.-I.; Nagano, S.; Ishimori, K.; Watanabe, Y.; Morishima, I.; Egawa, T.; Kitagawa, T.; Makino, R. *Biochemistry* **1993**, *32*, 241.

(28) Traylor, T. G.; Kim, C.; Richards, J. L.; Xu, F.; Perrin, C. L. *J. Am. Chem. Soc.* **1995**, *117*, 3468.